Ann. Geophysicae 14, 976–985 (1996)

Annales Geophysicae

On long-term evolution of seasonal precipitation in southwestern Europe

F. Valero, F. J. Doblas, J. F. González

Departamento de Física de la Tierra, Astronomía y Astrofísica II, Facultad de Ciencias Físicas, Universidad Complutense de Madrid, 28040 Madrid, Spain

Received: 28 June 1995/Revised: 25 January 1996/Accepted: 19 April 1996

Abstract. Annual cycles in long time series of precipitation from sixteen southwest European observatories have been analysed using complex demodulation. The stations have been clustered into two distinct regions and a hybrid one. They are referred to as the southwestern Europe precipitation Atlantic regime (SEPAR) and the southwestern Europe precipitation Mediterranean regime (SEPMER), with the hybrid regime referred to in terms of the mean amplitude ratios between semiannual and annual rainfall components. Some evidence of linking between seasonal cycle harmonic amplitudes and the zonal circulation has been found for SEPAR stations and a more obscured relationship for the SEPMER region. Within the SEPAR region the strength of the relationship is diminished towards the north. A trend analysis of the amplitudes against time since 1920 has also been carried out and the results reveal a divergent pattern in trends between annual and semiannual component amplitudes for the SEPAR region. In fact, both an increasing annual-amplitude trend and a decreasing semiannual-amplitude trend are observed, in each case statistically significant. The fact that the seasonal cycle variability of rainfall in southwestern Europe becomes more sensitive southwards to changes in atmospheric zonal circulation over the North Atlantic might, in our opinion, be related to the swing of the circumpolar vortex.

1 Introduction

Thomson (1995) has recently pointed out the evidence of a worldwide link between winter-summer temperature contrast and the climate change induced by greenhouse gases. Taking into account the physical relationship between the difference in the amount of solar energy that the Earth receives in winter and summer and the amplitude of the annual cycle in temperature, he finds that the likely role of solar energy on the climatic change is not as important as might be thought. Furthermore, tracking the annual cycle, he shows that there exists a general drift in the timing of the seasons (the date of the beginning of a "meteorological" year), which began around the 1940s, just when human-induced greenhouse warming appears to become stronger. This idea is based on the natural drift of one day per century, derived from the precession of the Earth, in the timing of the annual cycle. He also found variations in the timing of the annual cycle by studying northern-hemisphere records from about 1940. Moreover, by analysing both the temperature records in selected locations and the temperature averaged over the northern and southern hemispheres, he was able to identify an anomalous phase difference which accumulates over time and may even lead to reverse the sign of the natural phase drift of the annual cycle. This result is important because, according to Tabony (1984), the temperature contrast between seasons is related to the amplitude and phase of the annual cycle through the first and second harmonics. Generally, since the annual cycle accounts for a very important fraction of total variance of most meteorological variables, its time variations may have a non-negligible impact on atmospheric variability and therefore act upon the intra-annual (seasonal) variability and the timing of the seasons.

Climate may change in a wide range of potentially serious ways other than global warming. Precipitation can be considered one of the principal climatic elements to detect some likely climate change. Its high variability in time and space yields a low signal-to-noise ratio. Thus, evidence for any climatic change in precipitation becomes more difficult to detect than, for instance, that for the temperature itself. In fact, distribution of precipitation within a zonal belt is highly non-uniform and forces one to study this climatic element in a more restricted spatial setting.

Much of the variability in the extratropical atmosphere is directly associated with internal instability and

Correspondence to: F. Valero

non-linearity. A quantitative assessment of seasonal variability in the extratropics in general, and in regions such as Europe in particular, must rely on results from observational studies. We know that regional, including zonally averaged, climate variations often do not match those of the globe as a whole. Several large-scale analyses of precipitation changes over the northern and southern land masses have been carried out (Bradley *et al.*, 1987; Díaz *et al.*, 1989). They have demonstrated that during the last few decades precipitation has tended to increase in the mid-latitudes, but decreases in the northern-hemisphere subtropics and generally increases throughout the southern hemisphere. However, these large-scale features contain considerable spatial variability. Southwestern Europe straddles mid-latitudes and subtropics, and so involves greater uncertainty in precipitation time and space patterns.

Annual cycle evolutions have often been studied through harmonic analysis applied on overlapping and non-overlapping data subsets (Manley, 1974; Smith, 1984). More recently, the use of powerful tools to handle variables with a very poor signal-to-noise ratio, such as precipitation, has been seen to be successful. A preliminary observational study on long-term seasonal evolution of precipitation is carried out in this paper by means of a powerful tool called complex demodulation. Estimates in time domain of amplitude and phase for a fixed-frequency signal are obtained in attempting to find out their corresponding time evolutions. The main advantage of our approach is, as was argued by Thomson (1995), that it is a method which is able to work even with quite noisy time series.

Section 2 describes the data sets used. Section 3 consists of a background review of complex demodulation. The main systematic and repeatable differences in the characteristics of amplitude and phase time series from the individual observatories are described in Sect. 4, and in Sect. 5 some comments and conclusions are highlighted.

2 Data

Sixteen long time series of monthly precipitation have been used in this paper. Table 1 lists the latitude and longitude coordinates (with negative values to the west of Greenwich meridian), the sampling period and the total number of missing data for each station as well as their proportion in percentage (in parenthesis). Twelve of them are observatories spread over the Iberian Peninsula and the Balearic Islands. The other four observatories are sited over southwestern Europe. Two of them, Bordeaux and Marseille, have been reconstructed from several original recorded time series, provided by Météo-France, using the Durbin-Watson method described in Valero *et al.* (1996).

One important consideration in the selection of time series for analysis is the amount and distribution of missing data. After examination of the available datasets and the distribution of missing values in these datasets, some information about this issue is shown in Table 1. Some of the series contained gaps, but these did not exceed 3% of the total data in any case. Missing data become a lesser problem when the gaps are well scattered, as is the case here. Each missing datum was interpolated by averaging data for the same month of the three years previous to and three years following the gap. This procedure has a drawback in the case when gaps exist within a 3-year data segment either at the beginning or at the end of the record. In such a case, some data of the segment have been necessarily excluded.

Table 1. List of stations where monthly precipitation records have been studied. The table contains the geographic coordinates (latitude and longitude) and the first and last year of the studied period. The extreme right-hand side column denotes the total number of missing data as well as its percentage (in parenthesis)

Station	Lat.	Long.	Period	Missing data
Alicante (AL)	38°22′	− 0°30′	1899–1993	3 (0.3)
Badajoz (BA)	38°53′	− 6°58′	1899–1984	2 (0.2)
Bologna (BO)	44°°30′	11°18′	1813–1990	0 (0.0)
Bordeaux (BD)	44°25′	− 0°40′	1848–1994	0 (0.0)
Burgos (BU)	42°20′	− 3°42′	1899–1990	28 (2.6
Coruña (CO)	43°20′	− 8°25′	1899–1989	2 (0.2)
Granada (GR)	37°10′	− 3°42′	1899–1976	3 (0.3)
Jean (JA)	37°48′	3°48′	1899–1985	23 (2.2)
Madrid (MA)	40°25′	− 3°45′	1899–1991	2 (0.2)
Marseille (MS)	43°26′	5°12′	1749–1993	0 (0.0)
Milan (MI)	45°27′	9°11′	1764–1990	0 (0.0)
Murcia (MU)	37°59′	− 1°08′	1899–1980	14 (1.4)
Palma Mallorca (PM)	39°34′	2°39′	1899–1993	0 (0.0)
San Fernando (SF)	36°28′	− 6°12′	1899–1987	5 (0.5)
San Sebastian (SS)	43°19′	− 2°03′	1899–1994	0 (0.0)
Sevilla (SE)	37°23′	− 5°59′	1899–1993	17 (1.5)

Finally, the time series of mean sea-level pressure differences between Ponta Delgada, Azores and Akurery, Iceland from 1867 to 1989 has been tackled. This series can be viewed as an index of the North Atlantic oscillation (NAO) pattern (Rogers, 1984; Lamb and Peppler, 1987).

3 Estimating amplitude and phase

The signal processing method known as complex demodulation can be applied to any time series. The aim of the complex demodulation is to extract information about a perturbed periodic component with slowly varying amplitude and phase. Such information consists of the time variation of the amplitude and phase of any non-stationary component of selected frequency. The analysis is similar to harmonic analysis in that the amplitude and phase are described, but different in that the amplitude and phase are determined only by the data in a local time interval rather than by the whole series. An excellent description of complex demodulation is given by Bloomfield (1976).

For brevity, we shall only present the continuous-time formulation herein. A time series, $x(t)$, embedding an oscillation of ω frequency with a slow-time-varying amplitude and phase, $A(t)$ and $\Phi(t)$, respectively, can be expressed as:

$$x(t) = A(t)\cos(\omega t + \Phi(t)). \quad (1)$$

This oscillation may be merged with a noisy (non-periodical) term $R(t)$ without any component at frequency ω. In such a case, it can be rewritten as

$$x(t) = A(t)\cos(\omega + \Phi(t)) + R(t). \tag{2}$$

Complex demodulation consists mainly of two steps clearly illustrated by Humphries and Restrepo (1992). First, carrying out the shifting of the spectral density associated with the frequency ω to the zero frequency by multiplying the series $x(t)$ by $e^{-\omega t}$. Second, filtering out the resulting time series through a complex low-pass filter. Having applied this methodology, a new shifted and filtered complex time series $u(t)$ is obtained

$$u(t) = \int_{-\infty}^{+\infty} h(s)x(t-s)e^{-i\omega(t-s)}\,ds, \tag{3}$$

where $h(s)$ is the impulse response function of the filter or the weight function of the time-invariant linear system, which provides a description of the system in the time domain. The frequency response function $H(\omega)$ or transfer function is the Fourier transform of the impulse response function. This is a complex function and can be expressed as

$$H(\omega) = G(\omega)e^{i\gamma(\omega)}, \tag{4}$$

where $G(\omega)$ is the gain which is a measure of the changing amplitude of ω-frequency components and ranges between -1 and 1; $\gamma(\omega)$ is the phase shift. Note that if $R(t)$ has any frequency different from ω, it will be removed by the idealized low-pass filter in Eq. (3), because in this case $G(\omega)$ is a delta-shaped function.

Both amplitude and phase time series are given, respectively, by

$$A(t) = 2\|u(t)\|, \tag{5a}$$

$$\Phi(t) = \arg(u(t)), \tag{5a}$$

the operator $\|\ \|$ being the quadratic norm $[(\mathrm{Re}(u(t)))^2 + (\mathrm{Im}(u(t)))^2]^{1/2}$, and arg( ) the $tg^{-1}[\mathrm{Re}(u(t))/\mathrm{Im}(u(t))]$

Since in the current case the time series are discrete and of finite length, the low-pass filter ought to have a discrete impulse response function and hence a finite number of coefficients; that is to say, the theoretical frequency response function will have to be transformed into an empirical function with a maximum at ω. Accordingly, a frequency band rather than a single frequency is involved in the process (Enting, 1987). For $\Phi(t)$ not constant, two possibilities can arise. One is that either a linear fall or rise in time does occur. In this case, the signal frequency is not exactly determined but may still be obtained, as presented in Thomson (1995), by adding the initial frequency to the slope of the straight line fitted to the phase time series. On the other hand, the phase can vary almost randomly in time; here the variability results from those components $R(t)$ with frequencies very near to ω in Eq. (2) which are included within that spectral band inherent in the filter resolution. Fortunately, the variance of the 12- and 6-month period components is large enough when compared with the background noise.

In this paper, the least-square low-pass filter as defined in Bloomfield (1976) is used. The discrete impulse response function is given by

$$h_0 = \frac{\omega_c}{\pi},$$

$$h_u = \frac{\sin(u\delta)/2}{u\delta/2}\,\frac{\sin u\omega_c}{\pi u}, \tag{6}$$

where ω_c is the cutoff frequency and δ is the wavelength of the Gibbs-phenomenon (a characteristic of the truncated Fourier series of a discrete function) ripples originated by any discrete filter. The value of δ depends on the filter length k as

$$\delta(k) = 4\pi/(2k+1). \tag{7}$$

Most of the decay from the passband to the stopband in the gain takes place over a range of δ, and also depends inversely on filter length. Thus, the larger k is, the larger the rate of decaying is, thereby a lesser number of components close to ω are included in the filtering. With this filter the negative influence of the Gibbs phenomenon on the gain is greatly reduced and the phase $\gamma(\omega)$ kept unchanged. The advantage of this filter lies mainly in its behaviour near $\omega = 0$, where the gain is close to 1 (ensuring that virtually all the signal is passed) and slowly varying (so that different frequencies contributing to the peak are treated equivalently).

Features of the filter are given by two parameters: (i) the pass frequency ω_p (last frequency with gain equal to 1), and (ii) the stop frequency ω_s (first frequency with gain equal to 0).

4 Results and discussion

Complex demodulation is used here to analyse the presumed changes in amplitude and phase of seasonal precipitation cycle during the current century of 16 long monthly rainfall records.

An inspection of monthly rainfall periodograms in Fig. 1 reveals the annual cycle in two main ways or spectral modes: a first spectral mode for the case where 12-month component exceeds 6-month component (as depicted in Fig. 1a), and a second mode for the case in which 6-month component exceeds 12-month component (as depicted in Fig. 1b). The first and second harmonics account for most of the annual variance, in good agreement with the results of the comprehensive study of Hsu and Wallace (1976).

By observing in detail the first and second columns in Table 2, the stations may reasonably well be clustered in terms of each spectral mode or, analogously, by means of the ratios between semiannual and annual amplitude components. Those stations associated with ratios equal or greater than 1 obey a southwestern Europe precipitation Mediterranean regime (SEPMER), and those having a ratio lower than 1 are classified as being in a southwestern Europe precipitation Atlantic regime (SEPAR). For practical purposes, stations were clustered according

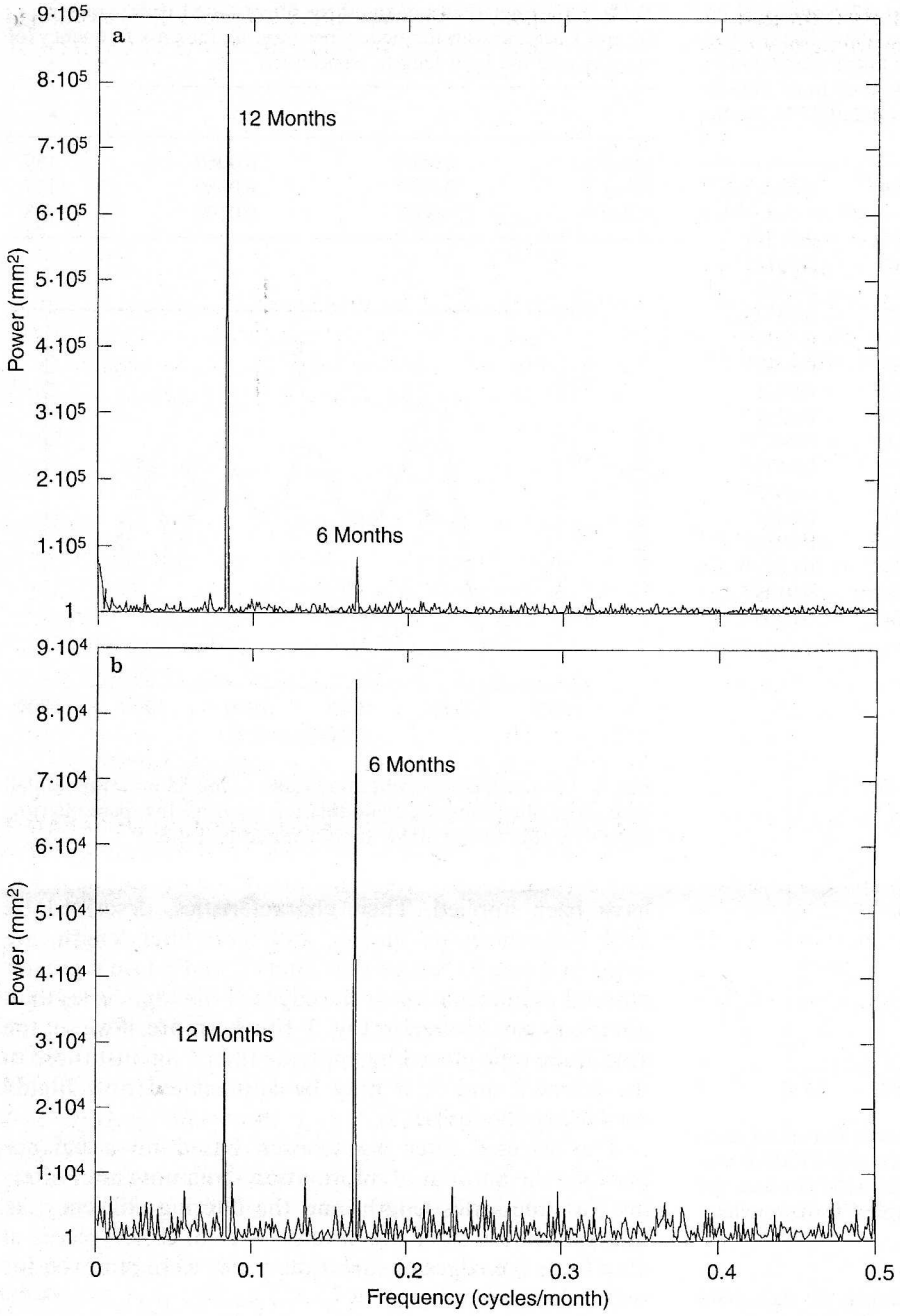

Fig. 1a, b. Periodogram of the **a** Coruña and **b** Murcia monthly rainfall time series. The 12- and 6-month periodicities stand out as peaks in the spectrum

to three major categories in terms of ratio values, namely:
- ratios less than or equal to 0.85 (SEPAR),
- ratios from 0.86 to 0.99 and
- ratios greater than 1 (SEPMER).

The threshold value of 0.85 was set in accordance with the issues derived from a comprehensive factor analysis of Iberian precipitation by Villa *et al.* (1985). Such a critical value was obtained by "tuning" ratio values so that SEPAR and SEPMER rainfall patterns were really much the same as those from Villa *et al.* (1985). By doing so, two stations, Madrid (MA) and Marseille (MS) (denoted by open circles in Fig. 2), exhibit a somewhat mixed pattern. Also in Fig. 2, ratios lower than 0.85 (solid circles) are found over much of the Iberian Peninsula and southwestern France associated with SEPAR-type stations, whereas ratios greater than 1 (solid triangles) linked to SEPMER-type stations fill southeastern Spain and northern Italy. There are two stations which do not exhibit the expected pattern: Burgos (BU), which is SEPMER instead of SEPAR as might have been expected, and Palma (PM), which SEPAR instead of SEPMER.

Ratios lower than 0.85 are representative of annual courses with only one wet and one dry season. It is evident that when the annual component is remarkably superior to the semiannual component, only a maximum and a minimum occur. In a similar manner, when ratios are greater than 1, rainfall throughout a year may be decomposed into both two wet and dry seasons.

Table 2. The averaged amplitudes (in mm) for 12-month and 6-month period components are listed in the first column. The two last columns show the slopes (in mm/month) of the linear regression in time for both 12- and 6-month component amplitude from 1920 to the end of the record. Significant slopes at the nominal 0.1% significance level are marked by *asterisks*

Station	12-months	6-months	Slope (12)	(Slope (6)
AL	9.8	22.8	−0.0024*	0.0102*
BA	27.7	11.2	0.0182*	−0.0083*
BO	10.7	20.3	−0.0038*	−0.0016
BD	18.4	11.6	0.0024*	−0.0043*
BU	10.8	12.6	0.0044*	−0.0136*
CO	42.0	13.2	0.0109*	−0.0097*
GR	24.4	13.4	0.0162*	−0.0021
JA	37.7	13.4	0.0078*	−0.0261*
MA	13.8	13.3	0.0076*	−0.0072*
MS	21.4	21.6	−0.0005	−0.0176*
MI	13.1	20.9	0.0034*	−0.0072*
MU	7.8	13.7	−0.0051*	0.0019
PM	18.8	15.9	−0.0078*	−0.0036*
SF	43.4	14.0	0.0224*	−0.0047*
SS	34.6	21.0	−0.0087*	−0.0139*
SE	38.8	13.5	0.0184*	−0.0203*

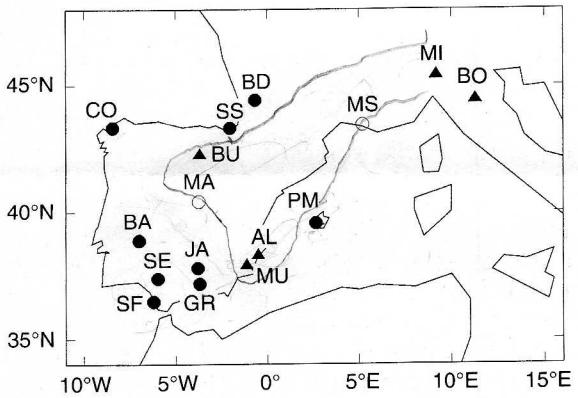

Fig. 2. Geographical arrangement of southwestern European rainfall spectral modes. First (SEPAR stations), second (SEPMER stations) and hybrid spectral modes are denoted by *solid circles*, *solid triangles*, and *open circles*, respectively. See Table 1 for acronyms

In indication of the skill of the clustering we can note that, for instance, Alicante (AL) and Murcia (MU) observatories show very high ratios (about equal to or greater than 2) against the Granada (GR) station which shows a ratio markedly lower than 1. This result agrees well with the issues argued by Valero *et al.* (1993) in a more locally detailed study conducted for southeastern Spain using cross-spectral analysis. After searching for the influence of the Atlantic climate along the Mediterranean coast, they have showed a progressive change along the coast line in the ratio between the spectral densities associated with the two aforementioned harmonics.

The complex demodulation of the precipitation series, was carried out using a variety of low-pass filter lengths. To evaluate the performance of low-pass filtering in extracting the yearly range of the annual cycle, San Sebastian's (SS) rainfall time series was chosen because no missing data exist within it. Three different low-pass filters

Table 3. Characteristics of the three filters tested in this paper. ω_s, ω_p and k are the stop-frequency (per month), the pass-frequency (of month), and the filter length, respectively

	ω_s	ω_p	k
Filter 1	0.0007	0.0060	189
Filter 2	0.0007	0.0080	137
Filter 3	0.0007	0.0100	108

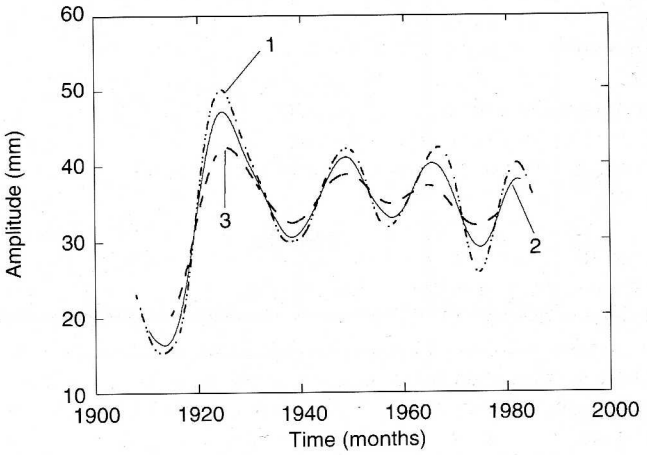

Fig. 3. 12-month component amplitudes of the SS monthly rainfall time series after complex demodulation for three low-pass filtering. Characteristics of the filters are illustrated in Table 3

have been applied. Their characteristics, described by their frequencies ω_p and ω_s and their filter length, are listed in Table 3. Notice that filters 2 and 3 lose a greater amount of information at the edges of the time series than filter 1, as can be seen in Fig. 3. Furthermore, if we set the amplitude reproduced by applying filter 1 against those of the filters 2 and 3, it may be appreciated how highly oscillatory the former is.

The selected filter was chosen based on a balance between the amount of information remaining after filtering (or time-series length) and the filtering efficiency, so that the chosen filter was filter 2. A total of 136 pieces of data from the edges of each time series were removed for such a low-pass filter.

4.1 Annual component

As can be seen in Fig. 4, the amplitudes of the 12-month precipitation component do not present a uniform but rather a relatively high oscillatory behaviour throughout the studied time interval. Another general aspect is the amplitudes' greater variability in both time and space when compared with those of Thompson (1995) for the 12-month temperature amplitudes. Considering that the used filter is very similar to that in Thompson's paper, these differences in the range of amplitude variability should not entirely be attributed to the characteristics of our filter, but rather to the nature of precipitation data and the characteristics of the region under study. However, as stated in Sect. 3, the reader should bear in